Supplementary Materials: Surface Oxidation of Supported Ni Particles and Its Impact on the Catalytic Performance during Dynamically Operated Methanation of CO_2

Benjamin Mutz [1,2], Andreas Martin Gänzler [1], Maarten Nachtegaal [3], Oliver Müller [4,5], Ronald Frahm [4], Wolfgang Kleist [1,2,6] and Jan-Dierk Grunwaldt [1,2,*]

[1] Institute for Chemical Technology and Polymer Chemistry, Karlsruhe Institute of Technology (KIT), D-76131 Karlsruhe, Germany; benjamin.mutz@kit.edu (B.M.); andreas.gaenzler@kit.edu (A.M.G.)
[2] Institute of Catalysis Research and Technology, Karlsruhe Institute of Technology (KIT), D-76344 Eggenstein-Leopoldshafen, Germany
[3] Paul Scherrer Institute (PSI), CH-5232 Villigen, Switzerland; maarten.nachtegaal@psi.ch
[4] Department of Physics, University of Wuppertal, D-42119 Wuppertal, Germany; omueller@slac.stanford.edu (O.M.); frahm@uni-wuppertal.de (R.F.)
[5] Stanford Synchrotron Radiation Lightsource (SSRL), SLAC National Accelerator Laboratory, Menlo Park, CA 94025, USA
[6] Laboratory of Industrial Chemistry, Ruhr-University Bochum, D-44801 Bochum, Germany; wolfgang.kleist@rub.de (W.K.)
* Correspondence: grunwaldt@kit.edu; Tel.: +49-721-608-42120

Received: 1 August 2017; Accepted: 5 September 2017; Published: date

1. Characterization data

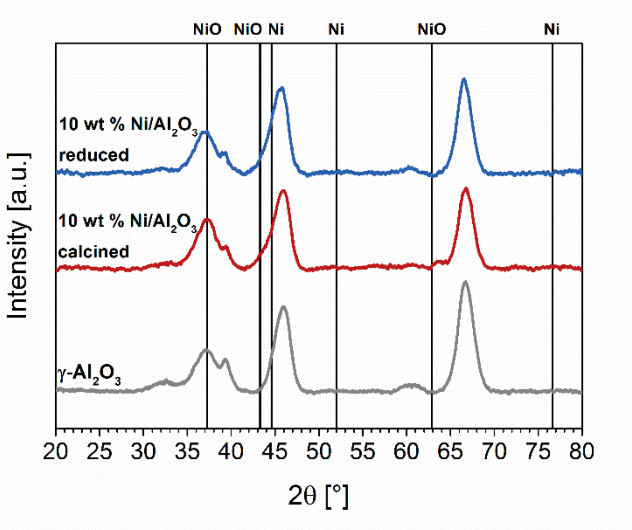

Figure S1. XRD patterns of the γ-Al_2O_3 support (grey) calcined at 600°C (4 h, 5 K/min), the 10 wt% Ni/Al_2O_3 catalyst (green) prepared by deposition precipitation and calcined at 500 °C (4 h, 5 K/min) in static air and the catalyst in the reduced state (red) after treatment in 50 % H_2/N_2 flow at 500 °C (2 h, 5 K/min) measured *ex situ*.

Only signals of the support (γ-Al_2O_3) are found in the X-ray patterns. Ni particles are X-ray amorphous and, thus, no structural information on the Ni particles (size oxidation state) can be derived.

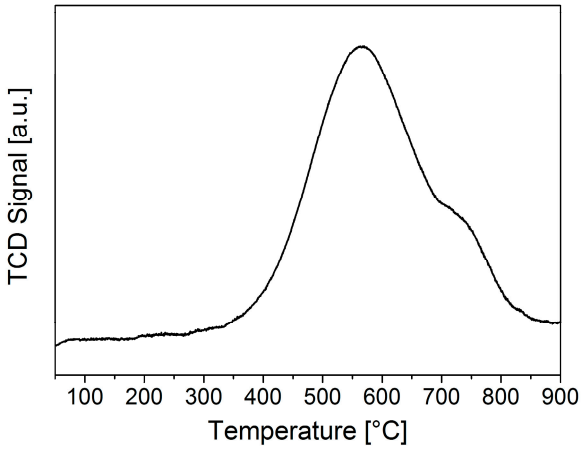

Figure S2. H_2-TPR profile of the 10 wt% Ni/Al_2O_3 catalyst using 10% H_2/Ar (50 mL/min, 100 mg sample), ramp rate 10 K/min.

The TPR profile with one main peak at 565 °C indicates a uniform particle size and the absence of agglomerates (should appear at lower temperatures). The small shoulder at higher temperatures might be due to $NiAl_2O_4$ with Ni being incorporated.

2. XAS data evaluation

2.1. Linear combination analysis (LCA)

To evaluate the Ni oxidation state during the experiment a linear combination of reference spectra was conducted to the respective sample spectra.

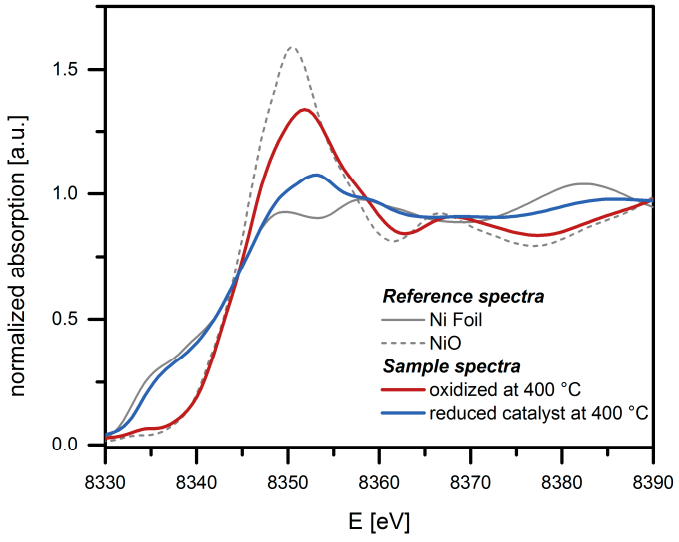

Figure S3. Reference XANES spectra of the bulk materials (recorded at room temperature) and *in situ* oxidized and reduces spectra of the catalyst (measured at 400 °C) for linear combination analysis (LCA).

In Figure S3 XANES spectra of the catalyst are presented along data obtained on reference samples: Ni-Foil with an oxidation state of zero and NiO with nickel in the oxidation state of +2. The pronounced feature around 8350 eV is called white-line and its extent strongly depends on the Ni oxidation state. The depicted sample spectra show the catalyst with Ni in the highest and lowest oxidation state. Since the *operando* XAS experiment was performed at 400 °C, the catalyst sample oxidized *in situ* in 5% O_2 and the corresponding XANES spectra at 400 °C was used as oxidized reference during the LCF analysis. As reduced reference the XANES spectrum acquired at 400 °C of the reduced catalyst was chosen. As shown in Figure S3 and also the EXAFS fitting data (Table S1 and S2) the Ni component did not fully

reduce due to the nature of the very small nanoparticles present in the catalyst and the intimate contact with the support (see also TPR-profile). Note furthermore, that the XAS spectrum is also dependent on the Ni particle size.

2.2. Reduced catalyst in He

Figure S4 shows the XANES and the FT EXAFS spectra of the reduced catalyst (at 500 °C in 50% H_2/He) in hydrogen atmosphere at room temperature and after heating again to 400 °C, and after the feed was switched to He. The Ni component was found stable in He atmosphere.

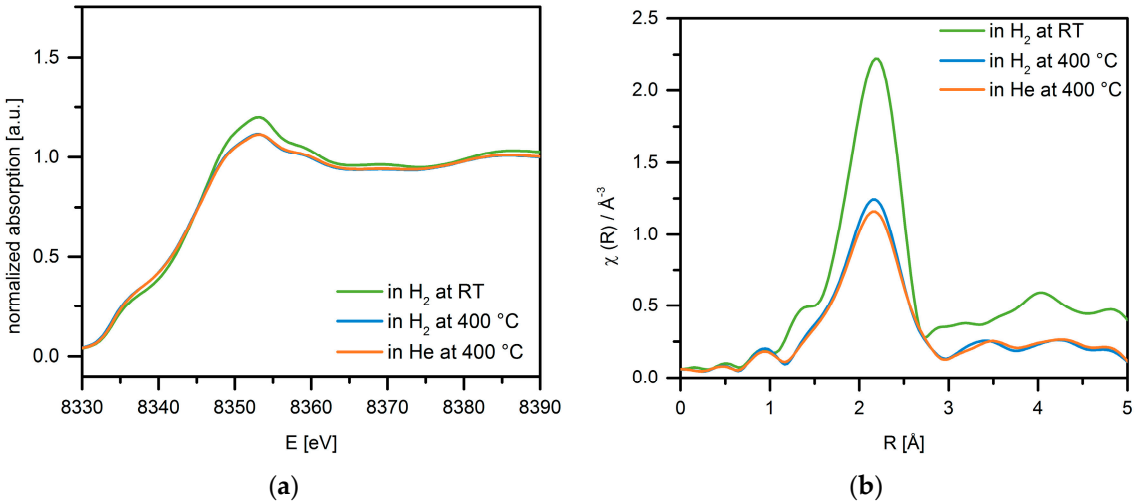

Figure S4. XANES and FT EXAFS spectra of the reduced catalyst in H_2/He at room temperature (RT) and at 400 °C and in He atmosphere at 400 °C.

2.3. Results of EXAFS fitting analysis

Table S1. Structural parameters of the local Ni atomic environment extracted from EXAFS spectra at the Ni K-edge of various samples measured at room temperature. Spectra of Ni foil and NiO references (measured as pellets) were used to obtain experimental amplitude reduction factors (Ni S_0^2 = 0.91, NiO S_0^2 = 0.92). Furthermore, the results for the calcined catalyst and after reduction at 500 °C are presented. The experimental and simulated EXAFS data are shown in Figure S8 and S9 together with the fitting ranges.

Sample (Condition)	**Atom**	**N**	**R (Å)[a]**	**σ^2 ×10^{-3} (Å^2)**	**ΔE_0 (eV)**	**ρ (%)**
Ni foil	Ni	12[f]	2.49	6.5 ± 0.3	7.2 ± 0.5	0.14
k-range: 3–13	Ni	6[f]	3.52	8.8 ± 0.6		
R-range: 1–5	Ni	24[f]	4.31	8.8 ± 0.6		
N^{ind}= 25; N^{var}=6	Ni	12[f]	4.97	8.8 ± 0.6		
NiO	O	6[f]	2.08	7.2 ± 2.1	-2.9 ± 0.6	0.48
k-range: 3–13	Ni	12[f]	2.97	8.0 ± 0.9		
R-range: 1–3						
N^{ind}= 12; N^{var}=5						
Sample at room temperature						

A: calcined pellet	O	5.0 ± 0.2	2.04 ± 0.01	5.5 ± 2.1	-4.6 ± 0.7	0.19
k-range: 3–12	Ni	5.1 ± 0.4	2.97 ± 0.01	10.5 ± 4.3		
R-range: 1–3.0						
N^{ind}= 11; N^{var}=5						
B: reduced	O	2.5 ± 0.2	2.03 ± 0.01	5.5 ± 2.1	8.2 ± 1.6	0.15
k-range:3–11	Ni	3.7 ± 0.3	2.49 ± 0.01	8.1 ± 0.1		
R-range:1–2.8	Ni	1.9 ± 0.7	2.97 ± 0.03	10.5 ± 4.3		
N^{ind}= 9; N^{var}=7						

f = value kept fixed during fitting procedure, a = fitted uncertainty 0.01 or lower, N = number of neighboring atoms, R = distance, σ^2 = mean square deviation of interatomic distance, ρ = misfit between experimental data and theory according to Ref [1].

Table S2. Structural parameters of the local Ni atomic environment extracted from EXAFS spectra at the Ni K-edge of various samples measured at room temperature and at 500 °C b before and after the presented experiments. They represent the most oxidizing and reducing states during the experiment. The experimental and simulated EXAFS data is shown in Figure S10 together with the fitting ranges.

Sample (Condition)	**Atom**	**N[a]**	**R (Å)[b]**	**σ^2 ×10^{-3} (Å^2)[c]**	**E_0 (eV)**	**ρ (%)**
Before 30 s H_2 drop-outs						
RT	O	2.0 ± 0.2	2.05 ± 0.01	5.5 [f]	10.5 ± 1.0	0.21
k-range: 3–10	Ni	4.7 ± 0.6	2.51 ± 0.01	8.1 ± 0.1		
R-range: 1.3–2.8						
N^{ind}= 6; N^{var}= 4						
500 °C	O	2.0 ± 0.2	2.03 ± 0.01	15.0 ± 3.3	7.7 ± 1.0	0.27
k-range:3–8.5	Ni	4.7 ± 0.6	2.48 ± 0.01	13.2 ± 1.5		
R-range:1.2–2.8						
N^{ind}= 5; N^{var}= 4						
After 30 s H_2 drop-outs						
500 °C	O	2.0 ± 0.3[l]	2.04 ± 0.02	15.0 ± 3.3	7.7 ± 1.9	0.12
k-range:3–8.5	Ni	4.9 ± 0.3	2.49 ± 0.01	13.2 ± 1.5		
R-range:1.2–2.8						
N^{ind}= 5; N^{var}= 4						
Before 300 s H_2 drop-outs (after 4 total 30 s modulation experiments)						
500 °C	O	1.5 ± 0.2	2.03 ± 0.01	15.0 ± 3.3	7.8 ± 1.3	0.04
k-range:3–8.5	Ni	5.4 ± 0.2	2.49 ± 0.01	13.2 ± 1.5 [b]		
R-range:1.2–2.8						
N^{ind}= 5; N^{var}= 4						
After 300 s H_2 drop-outs						
RT	O	1.5 ± 0.3	2.03 ± 0.02	5.5 [f]	8.5 ± 1.8	0.40
k-range: 3–10	Ni	5.7 ± 1.0	2.49 ± 0.01	8.1 ± 0.1		
R-range: 1.3–2.8						
N^{ind}= 6; N^{var}= 4						

500 °C	O	1.5 ± 0.3	2.03 ± 0.01	15.0 ± 3.3	7.8 ± 0.8	0.18
k-range:3–8.5	Ni	5.7 ± 1.0	2.48 ± 0.01	13.2 ± 1.5		
R-range:1.2–2.8						
N^{ind}= 5; N^{var}= 4						

N = number of neighboring atoms, R = distance, σ^2 = mean square deviation of interatomic distance, ρ = misfit between experimental data and theory, a = number of neighboring atoms constrained to be the same after each treatment at room temperature and 500 °C, f = value kept fixed during fitting procedure, b = fitted uncertainty 0.01 or lower, c =mean-square deviation constrained to be the same for respective temperature.

Table S3. Structural parameters of the local Ni atomic environment extracted from EXAFS spectra at the Ni K-edge of various samples measured at 400 °C. They represent the most oxidizing and reducing states during the experiment. The experimental and simulated EXAFS data is shown in Figure S11 together with the fitting ranges.

Sample (Condition)	**Atom**	**N**	**R (Å)[a]**	**σ^2 ×10^{-3} (Å^2)**	**E_0 (eV)**	**ρ (%)**
Oxidized in O_2	O	4.1 ± 0.3	2.05 ± 0.02	8.3 [f]	9.8 ± 1.3	0.30
k-range: 3–8.5	Ni	7.6 ± 0.8	2.97 ± 0.01	11.8[f]		
R-range: 1.1–3.2						
N^{ind}= 7; N^{var}=5						
After reaction (30 s modulation) at 400 °C in CO_2/H_2	O	2.2 ± 0.2	2.02 ± 0.03	8.3 [f]	7.5 ± 2.7	0.16
	Ni	2.4 ± 0.6	2.48 ± 0.02	11.4 ± 1.2 [f]		
	Ni	3.0 ± 0.8	2.94 ± 0.03	11.8 ± 2.1 [f]		
k-range: 3–9						
R-range: 1.2–2.9						
N^{ind}= 6; N^{var}=5						
After reaction (300 s modulation) at 400 °C in CO_2/H_2	O	3.0 ± 0.2	2.04 ± 0.03	8.3 [f]	8.4 ± 2.5	0.18
	Ni	1.9 ± 0.8	2.48 ± 0.02	11.4 ± 1.2 [f]		
	Ni	4.8 ± 0.9	2.97 ± 0.03	11.8 ± 2.1 [f]		
k-range: 3–9						
R-range: 1.2–2.9						
N^{ind}= 6; N^{var}=5						

f = value kept fixed during fitting procedure, a = fitted uncertainty 0.01 or lower, N = number of neighboring atoms, R = distance, σ^2 = mean square deviation of interatomic distance, ρ = misfit between experimental data and theory.

Table S4. Structural parameters of the local Ni atomic environment extracted from EXAFS spectra at the Ni K-edge of various samples measured at 400 °C during fluctuating methanation conditions during ***30 s H_2 dropouts***. The EXAFS data is extracted from the data set presented in Figure 4(a). They represent the most oxidizing and reducing states during the experiment. The data was Fourier transformed in the k-range 3–9 Å^{-1} and fitted within the R-range 1–3.2 Å. This resulted in 9 independent variables while 7 variables were fitted. The evaluated Ni and O coordination numbers are plotted in Figure 4(b). The experimental and simulated EXAFS data is shown in Fig S12.

Sample (Condition)	**Atom**	**N**	**R(Å)[a]**	**σ^2 ×10^{-3} (Å^2)**	**E_0 (eV)**	**ρ (%)**
Meth-6	O	1.6 ± 0.2	2.03 ± 0.2	8.3[f]	9.0 ± 1.5	0.27
k-range: 3–9	Ni	4.4 ± 0.3	2.49 ± 0.1	11.8[f]		
R-range: 1.2–3.2						
N^{ind}= 6; N^{var}=5						
Dropout-7	O	2.4 ± 0.2	2.02 ± 0.03	8.3[f]	7.6 ± 2.9	0.25
k-range: 3–9	Ni	2.0 ± 0.6	2.48 ± 0.02	11.4[f]		
R-range: 1.2–3.2	Ni	3.4 ± 0.9	2.96 ± 0.03	11.8[f]		
N^{ind}= 6; N^{var}=5						
Meth-7	O	1.8 ± 0.2	2.01 ± 0.2	8.3[f]	6.4 ± 2.2	0.23
k-range: 3–9	Ni	3.2 ± 0.4	2.48 ± 0.1	11.4[f]		
R-range: 1.2–3.2	Ni	1.9 ± 0.6	2.95 ± 0.3	11.8[f]		
N^{ind}= 6; N^{var}=5						
Dropout -8	O	3.0 ± 0.2	2.04 ± 0.02	8.3[f]	8.9 ± 2.1	0.14
k-range: 3–9	Ni	1.3 ± 0.6	2.48 ± 0.03	11.4[f]		
R-range: 1.2–3.2	Ni	4.4 ± 0.7	2.97 ± 0.03	11.8[f]		
N^{ind}= 6; N^{var}=5						
Meth -8	O	2.2 ± 2.0	2.02 ± 0.03	8.3[f]	6.8 ± 2.9	0.23
k-range: 3–9	Ni	2.3 ± 0.6	2.48 ± 0.01	11.4[f]		
R-range: 1.2–3.2	Ni	3.1 ± 0.9	2.96 ± 0.03	11.8[f]		
N^{ind}= 6; N^{var}=5						
Dropout -9	O	3.4 ± 0.2	2.04 ± 0.02	8.3[f]	9.5 ± 2.0	0.13
k-range: 3–9	Ni	1.0 ± 0.7	2.48 ± 0.03	11.4[f]		
R-range: 1.2–3.2	Ni	4.9 ± 0.8	2.97 ± 0.02	11.8[f]		
N^{ind}= 6; N^{var}=5						
Meth -9	O	2.6 ± 0.2	2.03 ± 0.02	8.3[f]	8.1 ± 2.2	0.15
k-range: 3–9	Ni	1.9 ± 0.5	2.48 ± 0.01	11.4[f]		
R-range: 1.2–3.2	Ni	3.6 ± 0.7	2.96 ± 0.03	11.8[f]		
N^{ind}= 6; N^{var}=5						
Dropout -10	O	3.5 ± 0.2	2.05 ± 0.02	8.3[f]	9.8 ± 2.0	0.12
k-range: 3–9	Ni	0.9 ± 0.7	2.46 ± 0.03	11.4[f]		
R-range: 1.2–3.2	Ni	5.1 ± 0.8	2.98 ± 0.02	11.8[f]		
N^{ind}= 6; N^{var}=5						
Meth -10	O	2.8 ± 0.2	2.03 ± 0.03	8.3[f]	8.5 ± 2.2	0.16
k-range: 3–9	Ni	1.5 ± 0.6	2.48 ± 0.02	11.4[f]		
R-range: 1.2–3.2	Ni	4.1 ± 0.8	2.97 ± 0.03	11.8[f]		
N^{ind}= 6; N^{var}=5						

Dropout -11	O	3.6 ± 0.2	2.05 ± 0.02	8.3[f]	9.8 ± 1.9	0.11
k-range: 3–9	Ni	0.9 ± 0.7	2.46 ± 0.03	11.4[f]		
R-range: 1.2–3.2	Ni	5.2 ± 0.8	2.98 ± 0.02	11.8[f]		
N^{ind}= 6; N^{var}=5						
Meth -11	O	3.0 ± 0.2	2.04 ± 0.02	8.3[f]	8.8 ± 2.1	0.14
k-range: 3–9	Ni	1.5 ± 0.6	2.48 ± 0.02	11.4[f]		
R-range: 1.2–3.2	Ni	4.4 ± 0.8	2.97 ± 0.02	11.8[f]		
N^{ind}= 6; N^{var}=5						
Dropout -12	O	3.6 ± 0.2	2.05 ± 0.02	8.3[f]	9.8 ± 1.9	0.11
k-range: 3–9	Ni	0.8 ± 0.7	2.46 ± 0.04	11.4[f]		
R-range: 1.2–3.2	Ni	5.4 ± 0.8	2.97 ± 0.02	11.8[f]		
N^{ind}= 6; N^{var}=5						
Meth -12	O	3.1 ± 0.2	2.05 ± 0.03	8.3[f]	9.4 ± 2.4	0.20
k-range: 3–9	Ni	1.4 ± 0.7	2.48 ± 0.02	11.4[f]		
R-range: 1.2–3.2	Ni	4.4 ± 0.9	2.97 ± 0.03	11.8[f]		
N^{ind}= 6; N^{var}=5						
Dropout -13	O	3.7 ± 0.2	2.06 ± 0.03	8.3[f]	10.0 ± 2.1	0.15
k-range: 3–9	Ni	0.8 ± 0.8	2.46 ± 0.04	11.4[f]		
R-range: 1.2–3.2	Ni	5.3 ± 0.9	2.98 ± 0.03	11.8[f]		
N^{ind}= 6; N^{var}=5						
Meth -13	O	3.2 ± 0.2	2.05 ± 0.02	8.3[f]	9.5 ± 2.2	0.16
k-range: 3–9	Ni	1.3 ± 0.7	2.48 ± 0.04	11.4[f]		
R-range: 1.2–3.2	Ni	4.5 ± 0.8	2.97 ± 0.02	11.8[f]		
N^{ind}= 6; N^{var}=5						
Dropout -14	O	3.7 ± 0.2	2.06 ± 0.02	8.3[f]	10.0 ± 2.0	0.13
k-range: 3–9	Ni	0.8 ± 0.7	2.46 ± 0.04	11.4[f]		
R-range: 1.2–3.2	Ni	5.3 ± 0.8	2.98 ± 0.02	11.8[f]		
N^{ind}= 6; N^{var}=5						
Meth -14	O	3.2 ± 0.2	2.04 ± 0.02	8.3[f]	8.8 ± 1.8	0.10
k-range: 3–9	Ni	1.1 ± 0.6	2.47 ± 0.02	11.4[f]		
R-range: 1.2–3.2	Ni	4.8 ± 0.7	2.97 ± 0.02	11.8[f]		
N^{ind}= 6; N^{var}=5						

a = fitted uncertainty 0.01 or lower, f = fixed during fit, N = number of neighboring atoms, R = distance, σ^2 = mean square deviation of interatomic distance, ρ = misfit between experimental data and theory.

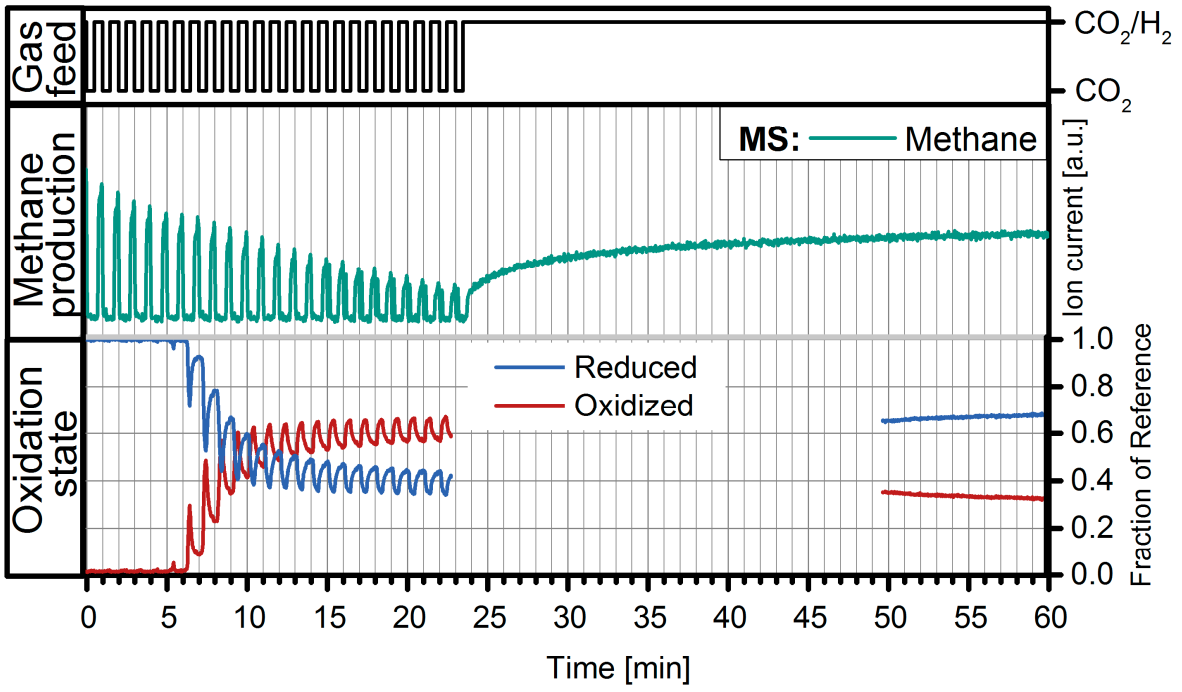

Figure S5. Full length of the experiment including 30 s modulation of methanation of CO_2 (H_2/CO_2 = 4) and CO_2 at constant WHSV of 12000 $mL_{CO2}/(g_{cat} \cdot h)$ and GHSV of 71700 h^{-1}. The figure shows the valve signal in the upper part (black), the CH_4 signal of the MS (m/z 15) in the middle part (green) and the fraction of reduced (blue) and oxidized (red) Ni from LCF of the XANES spectra according to the references in Figure S3.

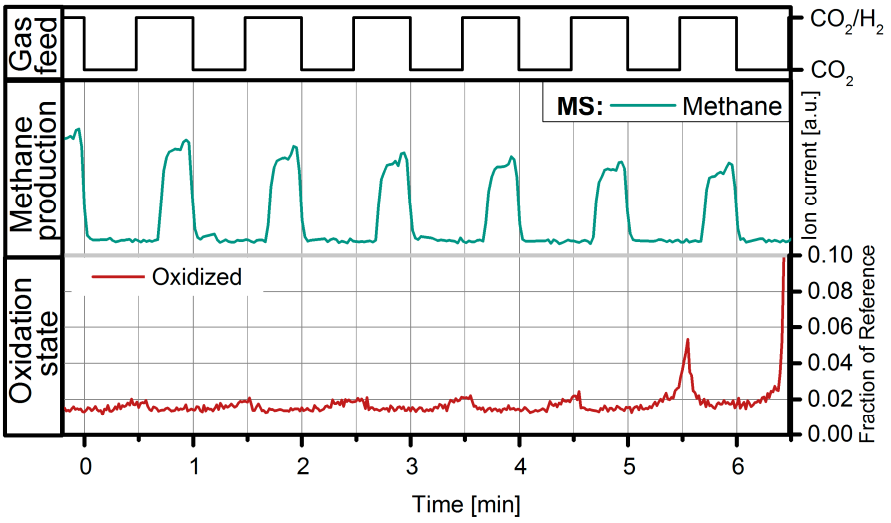

Figure S6. Zoom of first 6 min of the 30 s modulation of Figure S5.

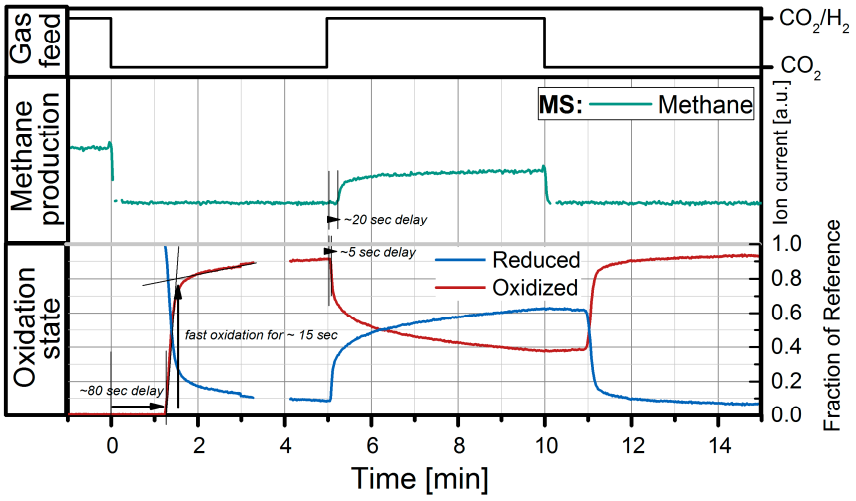

Figure S7. Zoom of the first 14 min of the 300 s modulation of methanation of CO_2 ($H_2/CO_2 = 4$) and CO_2 at constant WHSV of 12000 $mL_{CO2}/(g_{cat} \cdot h)$ and GHSV of 71700 h^{-1}. The figure shows the valve signal in the upper part (black), the CH_4 signal of the MS (m/z 15) in the middle part (green) and the fraction of reduced (blue) and oxidized (red) Ni from LCF of the XANES spectra according to the references in Figure S3.

Based on Figure S7 the amount of O_2 present in the experiment was estimated. We assume that the oxidation of Ni starts at the reactor inlet and the oxidation front propagates through the catalyst bed. XAS spectra were recorded in the middle of the catalyst bed. Therefore, half of the catalyst was oxidized to appox. 75% 95 s after the gas switch, as the fast increase in oxidation monitored by XAS declines. 3 µmol Ni was oxidized as the oxidation front reached the middle of the catalyst bed, necessitating an amount of 1.5 µmol O_2 which is approximately 1000 ppm O_2 of the 20 mL/min total gas flow.

Table S5. Structural parameters of the local Ni atomic environment extracted from EXAFS spectra at the Ni K-edge of various samples measured at 400 °C during fluctuating methanation conditions during ***300 s H_2 dropouts***. The EXAFS data is extracted from the data set presented in Figure 6 a). They represent the most oxidizing and reducing states during the experiment. The data was Fourier transformed in the k-range 3–9 $Å^{-1}$ and fitted within the R-range 1–3.2 Å. This resulted in 9 independent variables while 7 variables were fitted. The evaluated Ni and O coordination numbers are plotted in Figure 6(b). The experimental and simulated EXAFS data is shown in Figure S13 together with the fitting ranges.

Sample (Condition)	Atom	N	R(Å)	$\sigma^2 \times 10^{-3}$ (Å^2)	E_0 (eV)	ρ (%)
Meth -0	O	1.1 ± 0.2	2.03 ± 0.01	8.3 ± 1.5[b]	8.4 ± 2.0	0.22
k-range: 3–9	Ni	5.1 ± 0.3	2.49 ± 0.03	11.4 ± 1.2[b]		
R-range: 1.2–3.2						
N^{ind}= 6; N^{var}=5						
Meth -1	O	2.4 ± 0.2	2.03 ± 0.03	8.3 ± 1.5[b]	7.9 ± 2.5	0.27
k-range: 3–9	Ni	2.7 ± 0.6	2.48 ± 0.02	11.4 ± 1.2[b]		
R-range: 1.2–3.2	Ni	3.8 ± 0.8	2.96 ± 0.03	11.8 ± 2.1[b]		
N^{ind}= 6; N^{var}=5						
Meth -2	O	2.7 ± 0.2	2.03 ± 0.02	8.3 ± 1.5[b]	8.5 ± 2.0	0.11
k-range: 3–9	Ni	2.3 ± 0.6	2.48 ± 0.01	11.4 ± 1.2[b]		

R-range: 1.2-3.2	Ni	4.2 ± 0.7	2.96 ± 0.02	11.8 ± 2.1 [b]		
N^{ind}= 6; N^{var}=5						
Meth -3	O	2.9 ± 0.2	2.04 ± 0.03	8.3 ± 1.5 [b]	8.9 ± 2.3	0.16
k-range: 3–9	Ni	2.0 ± 0.7	2.48 ± 0.02	11.4 ± 1.2 [b]		
R-range: 1.2–3.2	Ni	4.6 ± 0.9	2.96 ± 0.03	11.8 ± 2.1 [b]		
N^{ind}= 6; N^{var}=5						
Meth -4	O	3.0 ± 0.2	2.04 ± 0.03	8.3 ± 1.5 [b]	9.0 ± 2.2	0.14
k-range: 3–9	Ni	2.0 ± 0.7	2.48 ± 0.02	11.4 ± 1.2 [b]		
R-range: 1.2–3.2	Ni	4.9 ± 0.8	2.97 ± 0.02	11.8 ± 2.1 [b]		
N^{ind}= 6; N^{var}=5						
Meth -5	O	3.0 ± 0.2	2.04 ± 0.01	8.3 ± 1.5 [b]	8.7 ± 2.3	0.14
k-range: 3–9	Ni	1.7 ± 0.7	2.48 ± 0.01	11.4 ± 1.2 [b]		
R-range: 1.2–3.2	Ni	5.1 ± 0.9	2.97 ± 0.01	11.8 ± 2.1 [b]		
N^{ind}= 6; N^{var}=5						
Meth -6	O	3.1 ± 0.2	2.04 ± 0.03	8.3 ± 1.5 [b]	9.0 ± 2.2	0.14
k-range: 3–9	Ni	1.8 ± 0.7	2.48 ± 0.02	11.4 ± 1.2 [b]		
R-range: 1.2–3.2	Ni	5.0 ± 0.8	2.97 ± 0.02	11.8 ± 2.1 [b]		
N^{ind}= 6; N^{var}=5						
Meth -7	O	3.1 ± 0.2	2.04 ± 0.03	8.3 ± 1.5 [b]	9.3 ± 2.3	0.16
k-range: 3–9	Ni	1.8 ± 0.7	2.48 ± 0.02	11.4 ± 1.2 [b]		
R-range: 1.2–3.2	Ni	5.0 ± 0.9	2.97 ± 0.03	11.8 ± 2.1 [b]		
N^{ind}= 6; N^{var}=5						
Meth -8	O	3.1 ± 0.2	2.05 ± 0.03	8.3 ± 1.5 [b]	9.0 ± 2.2	0.13
k-range: 3–9	Ni	1.6 ± 0.7	2.48 ± 0.02	11.4 ± 1.2 [b]		
R-range: 1.2–3.2	Ni	5.3 ± 0.9	2.97 ± 0.02	11.8 ± 2.1 [b]		
N^{ind}= 6; N^{var}=5						
Dropout -1-8	O	4.0 ± 0.2	2.05 ± 0.01	8.3 [f]	9.9 ± 0.9	0.27
k-range: 3–9	Ni	7.6 ± 0.5	2.96 ± 0.01	11.8[f]		
R-range: 1.2–3.2						
N^{ind}= 6; N^{var}=5						

[b] = mean-square deviation evaluated simultaneously spectra Red 0–8, f = fixed during fit, extracted from fit of Meth 0–8 during 300 s switches, N = number of neighboring atoms, R = distance, σ^2 = mean square deviation of interatomic distance, ρ = misfit between experimental data and theory according to Ref [1].

Ni - Foil

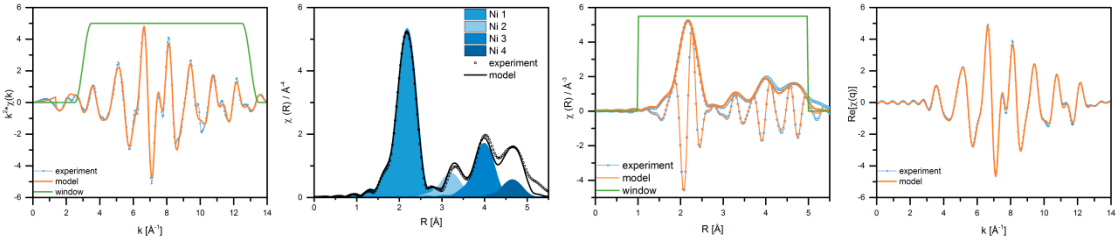

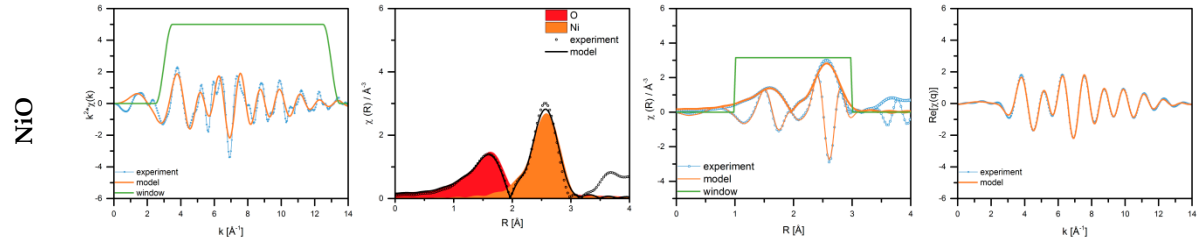

Figure S8. Experimental and simulated EXAFS data of reference data (Ni-Foil and NiO). From left to right: extracted EXAFS data in k-space with k-range used for data fitting; FT EXAFS data and respective components of the simulated data (magnitude of FT); magnitude and imaginary part of FT EXAFS data with R-range used for data fitting, real part of back FT data (R-range: 1–3.2 Å).

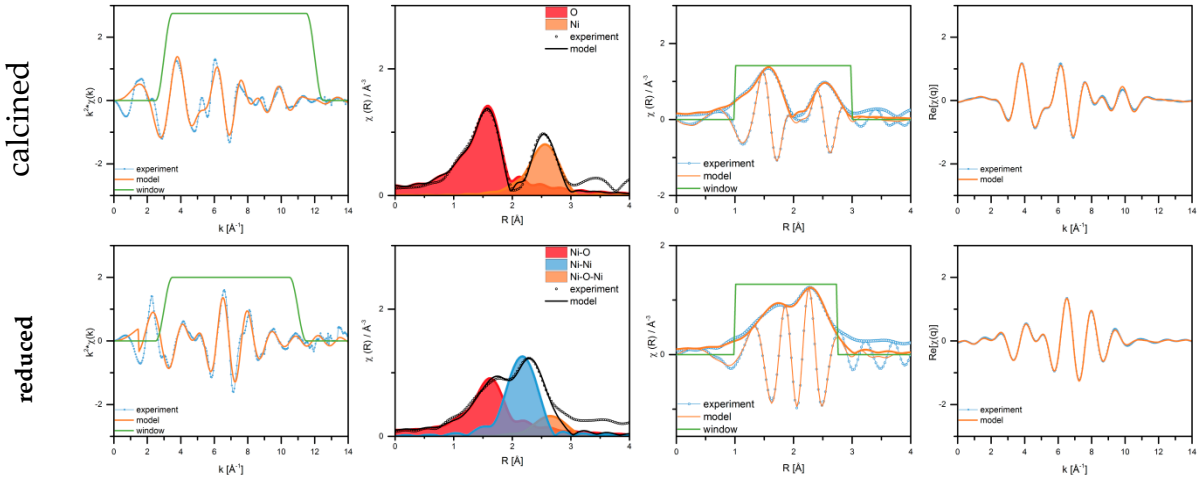

Figure S9. Experimental and simulated EXAFS data of the 10 wt% Ni/Al_2O_3 catalyst at room temperature. From left to right: extracted EXAFS data in k-space with k-range used for data fitting; FT EXAFS data and respective components of the simulated data (magnitude of FT); magnitude and imaginary part of FT EXAFS data with R-range used for data fitting, real part of back FT data (R-range: 1–3.2 Å).

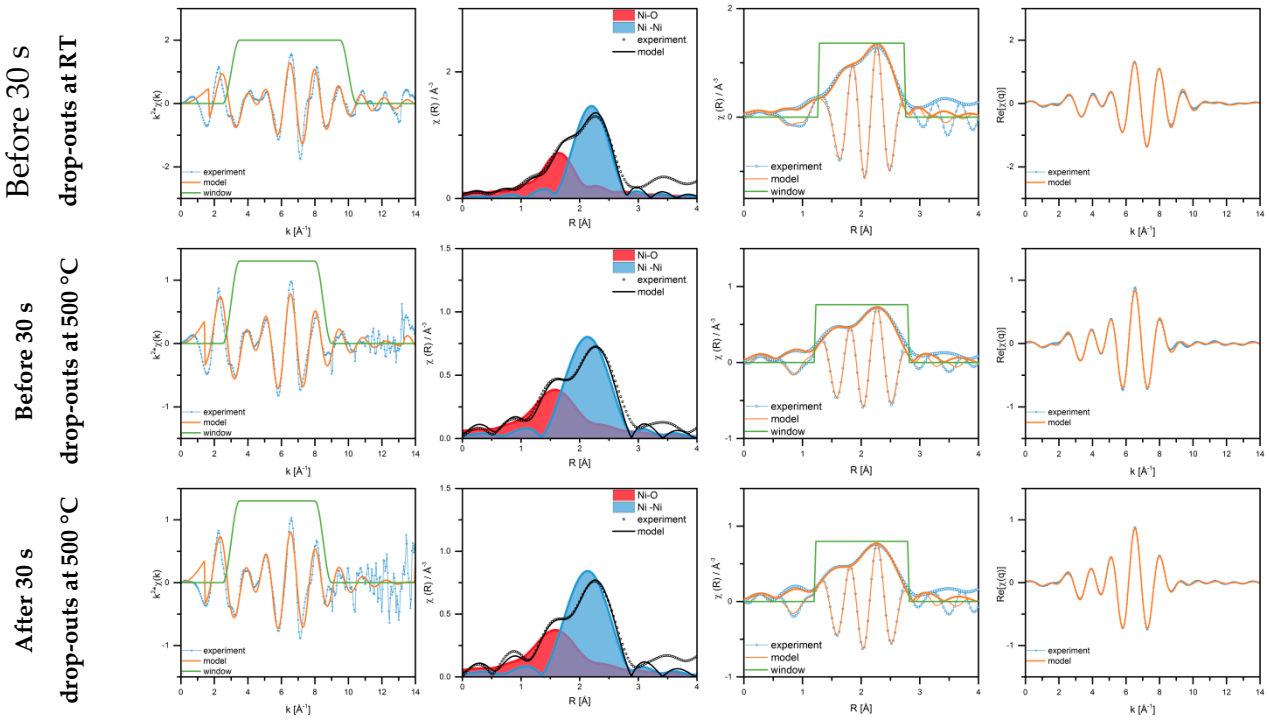

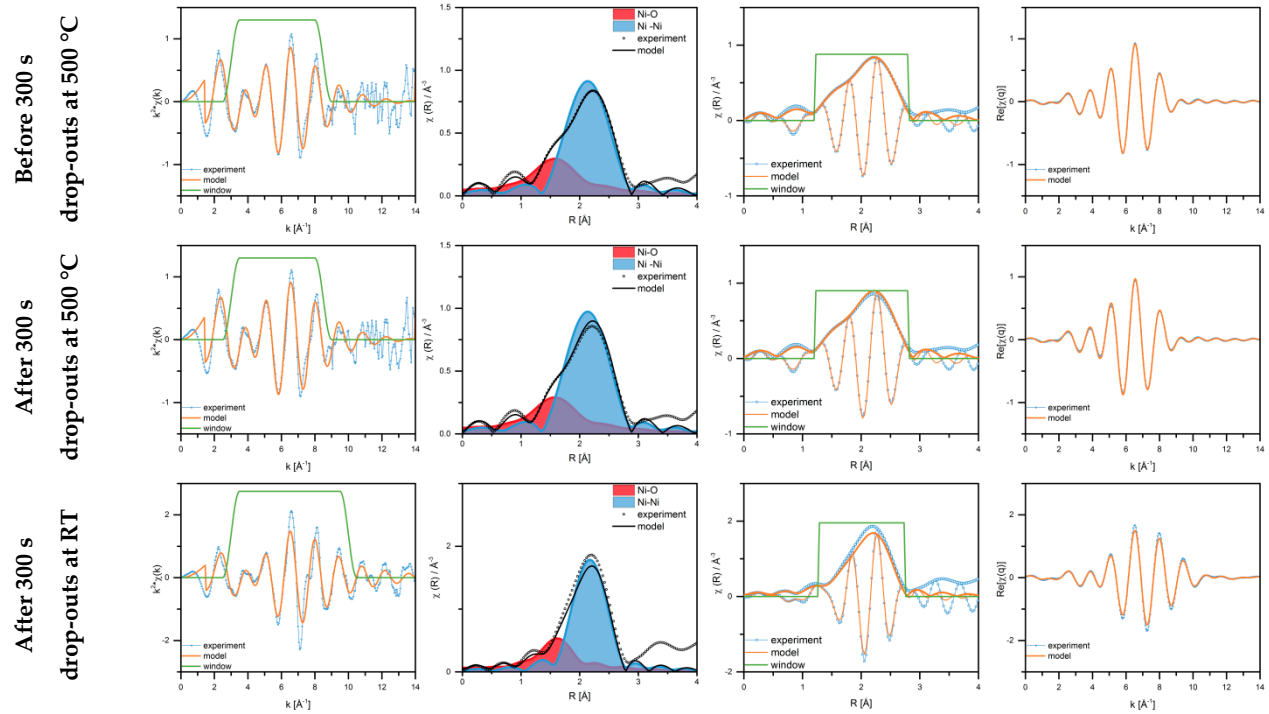

Figure S10. Experimental and simulated EXAFS data of the 10 wt% Ni/Al_2O_3 catalyst at room temperature. From left to right: extracted EXAFS data in k-space with k-range (see Table S3, k-weight = 2) used for data fitting; FT EXAFS data and respective components of the simulated data (magnitude of FT); magnitude and imaginary part of FT EXAFS data with R-range used for data fitting, real part of back FT data (see Table S3).

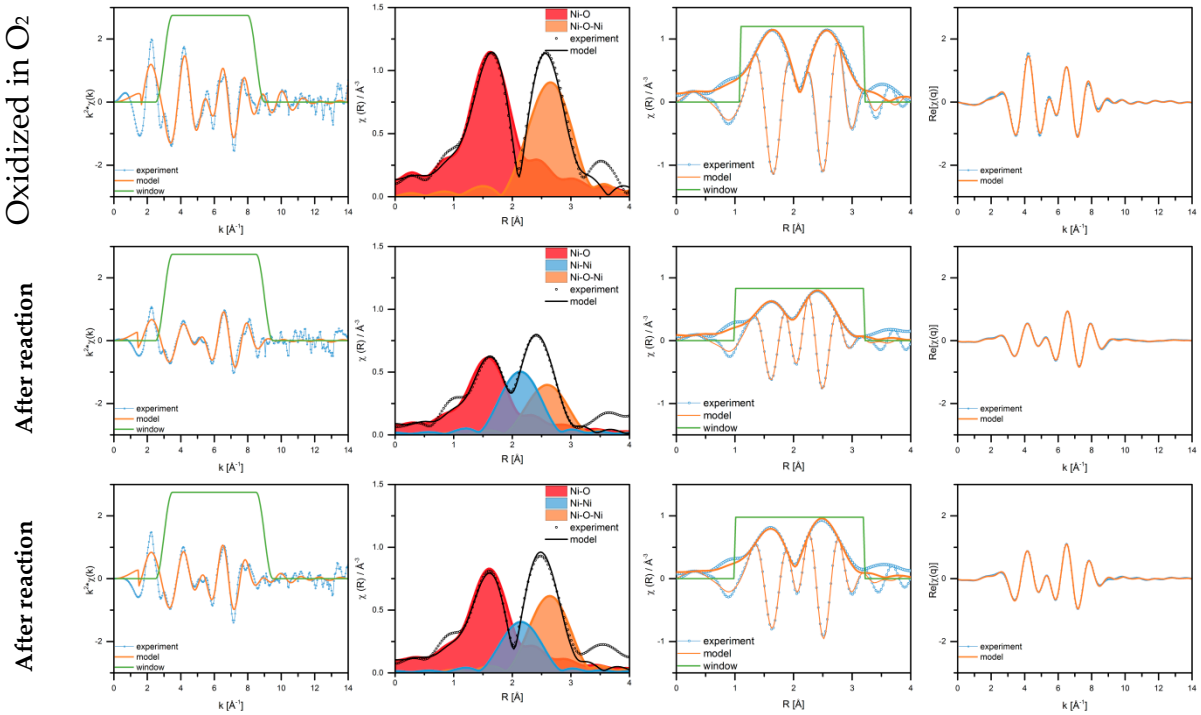

Figure S11. Experimental and simulated EXAFS data of the 10 wt% Ni/Al_2O_3 catalyst at 400 °C. From left to right: extracted EXAFS data in k-space with k-range used for data fitting (see Table S4, k-weight = 2); FT EXAFS data and respective components of the simulated data (magnitude of FT); magnitude and imaginary part of FT EXAFS data with R-range used for data fitting, real part of back FT data (see Table S4).

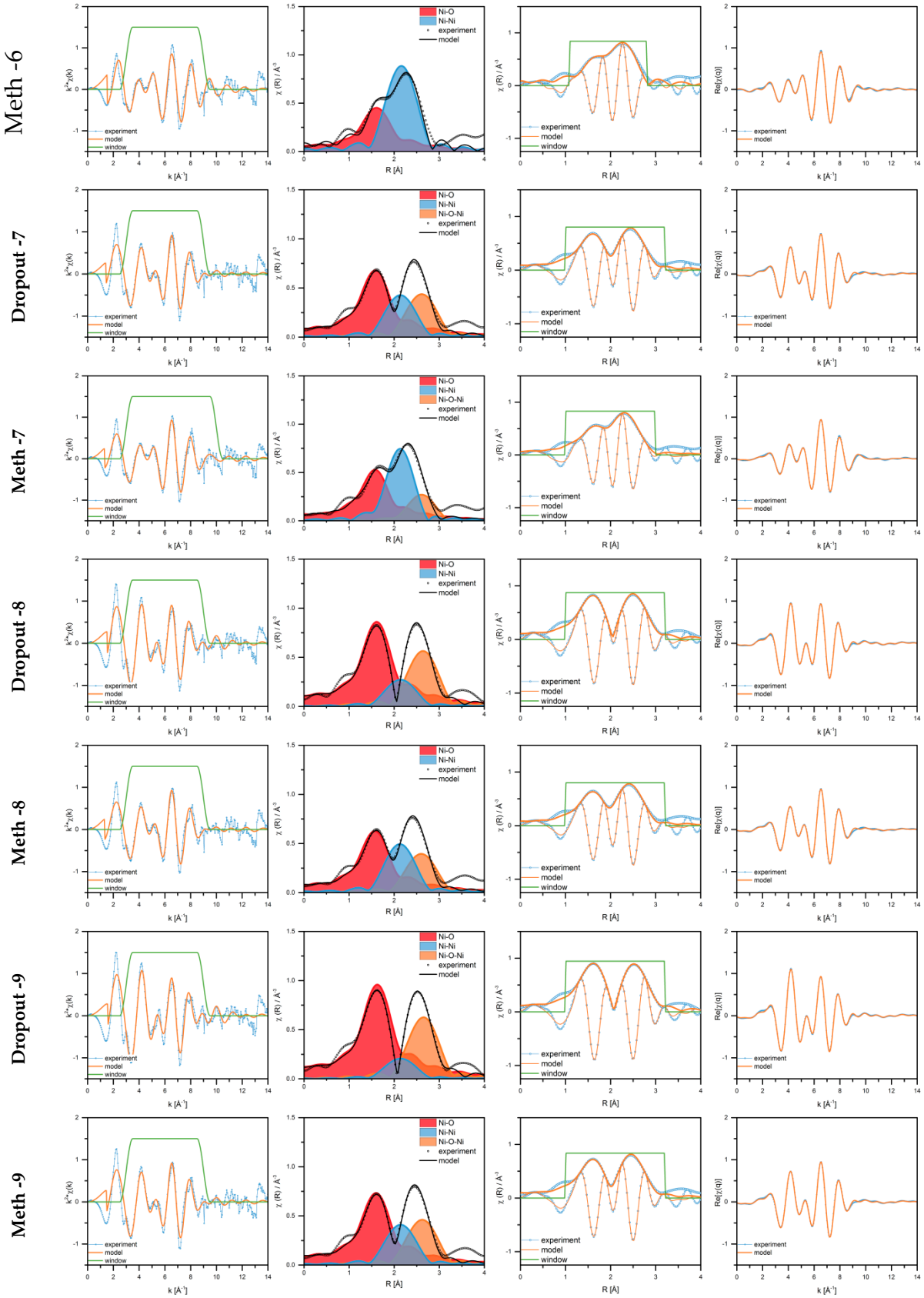
Meth -6
Dropout -7
Meth -7
Dropout -8
Meth -8
Dropout -9
Meth -9
Ni-O
Ni-Ni
Ni-O-Ni
experiment
model
window
k [Å^{-1}]
R [Å]
χ (R) / Å^3
Re[χ(q)]

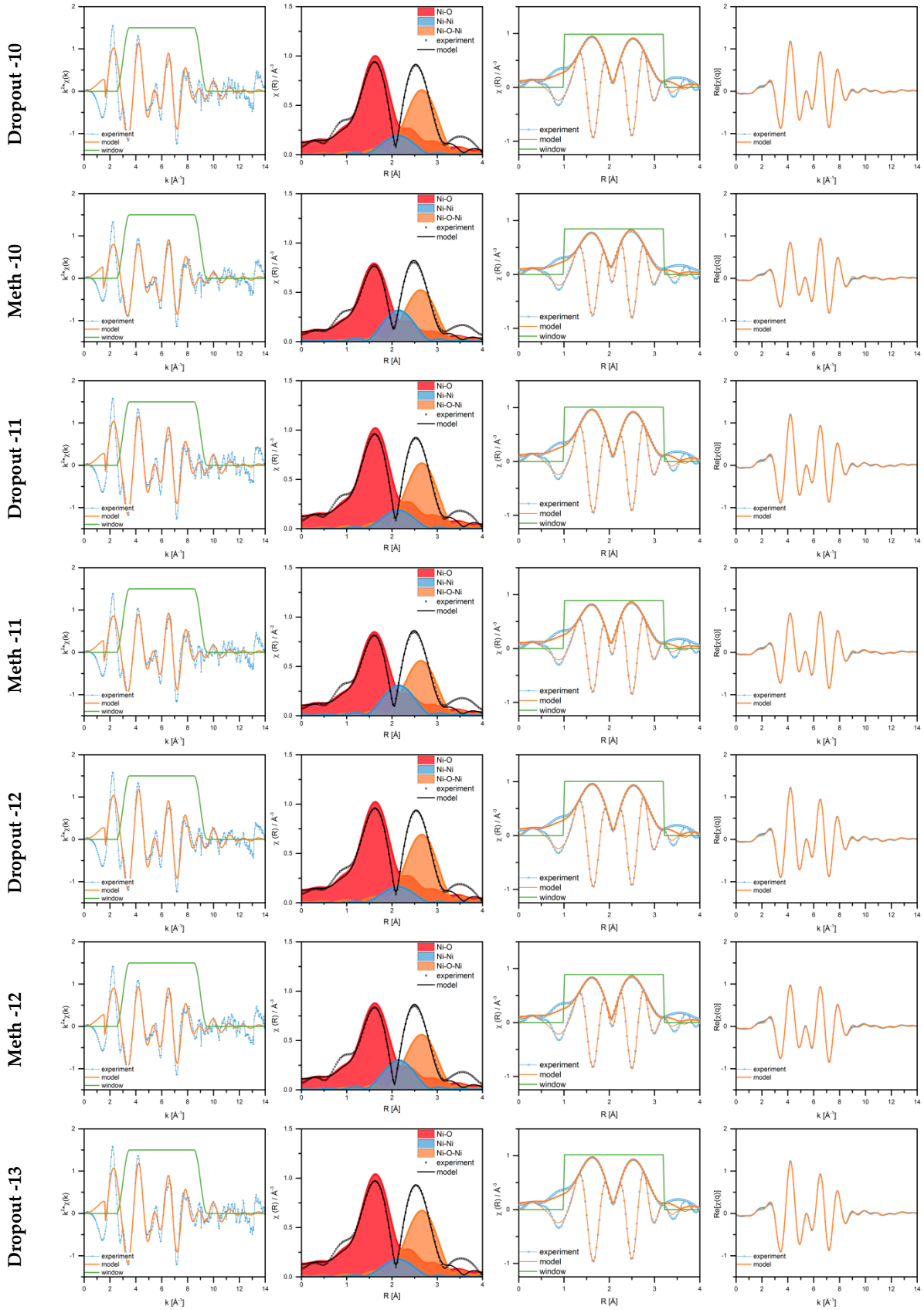
Dropout -10
Meth -10
Dropout -11
Meth -11
Dropout -12
Meth -12
Dropout -13
Ni-O
Ni-Ni
Ni-O-Ni
experiment
model
window
k [Å⁻¹]
R [Å]
χ (R) / Å⁻³
Re[χ(q)]

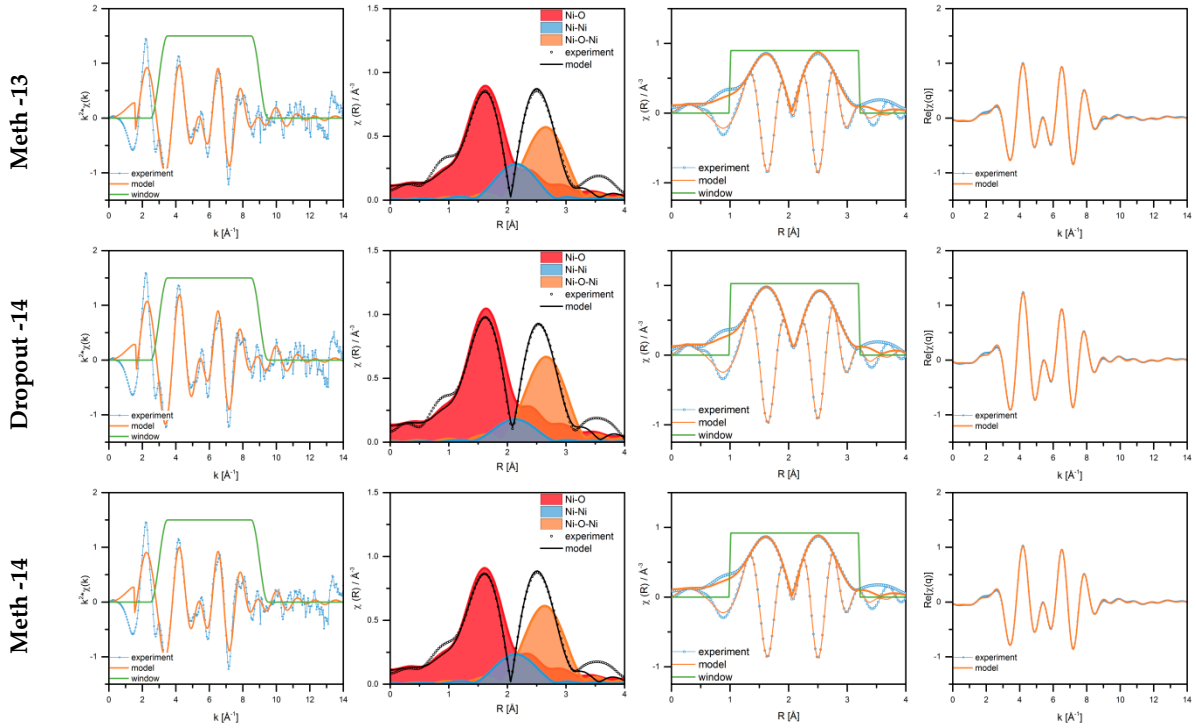

Figure S12. Experimental and simulated EXAFS data of the 10 wt% Ni/Al_2O_3 catalyst during methanation with *30 s H_2 dropouts*. From left to right: extracted EXAFS data in k-space with k-range used for data fitting (3–9 $Å^{-1}$, k-weight = 2); FT EXAFS data and respective components of the simulated data (magnitude of FT); magnitude and imaginary part of FT EXAFS data with R-range used for data fitting (see Table S3Å), real part of back FT data (R-range: 1–3.2 Å).

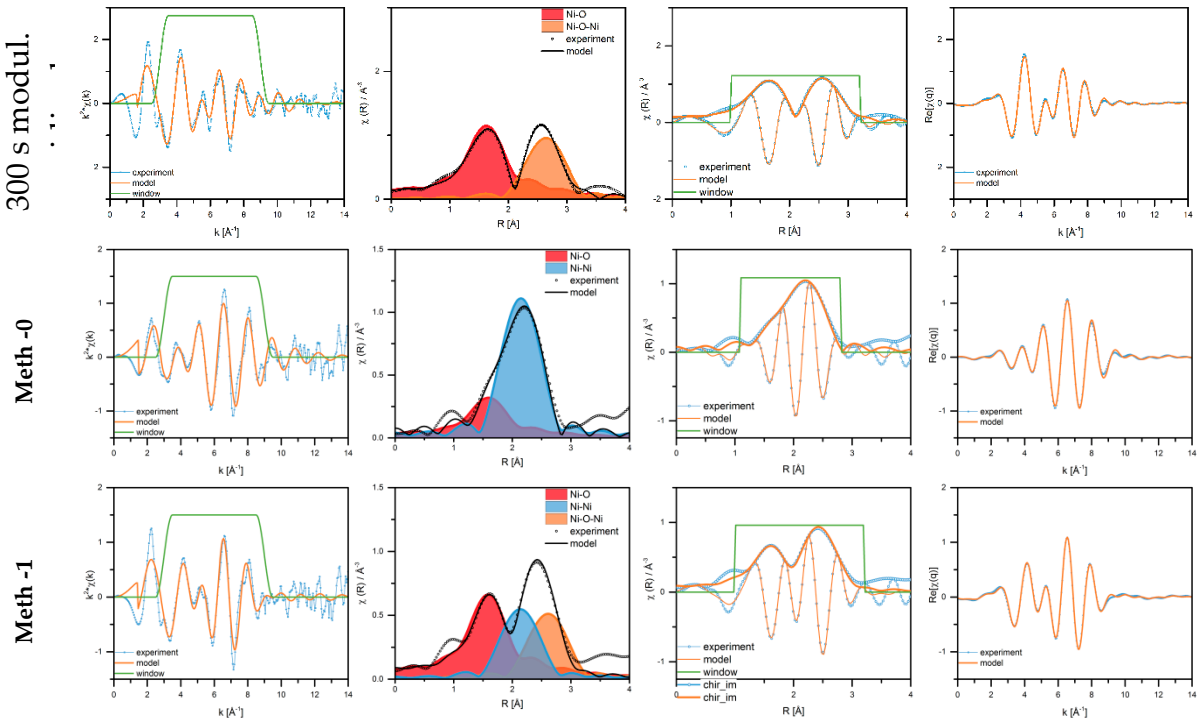

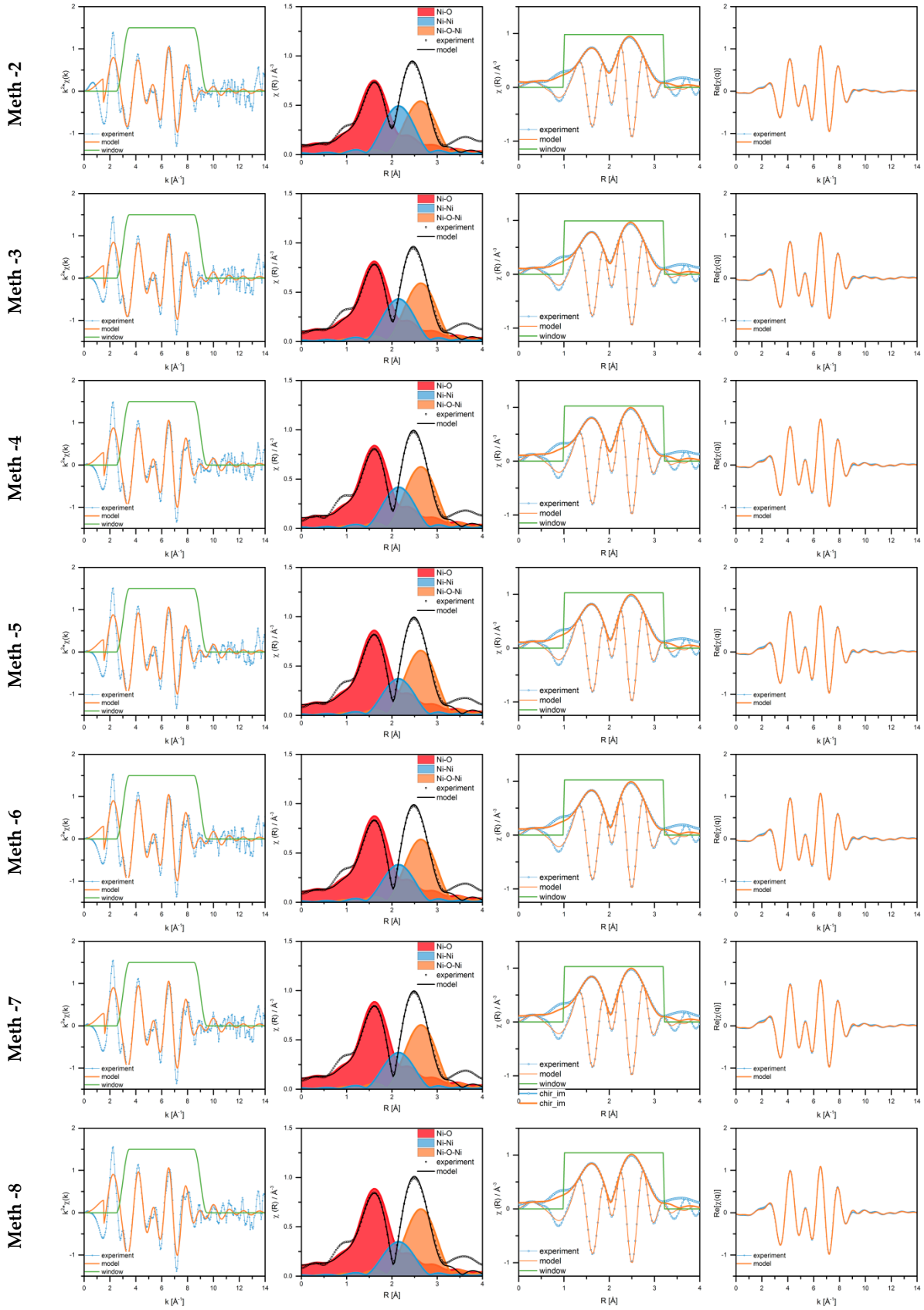

Figure S13. Experimental and simulated EXAFS data of the 10 wt% Ni/Al_2O_3 catalyst during methanation with *300 s H_2 dropouts*. From left to right: extracted EXAFS data in k-space with k-range used for data fitting (2–9 $Å^{-1}$, k-weight = 2); FT EXAFS data and respective components of the simulated data (magnitude of FT); magnitude and imaginary part of FT EXAFS data with R-range used for data fitting (1.2–2.9 Å), real part of back FT data (R-range: 1.2–3.2 Å).

3. Mass spectrometry data recorded during the QEXAFS experiments

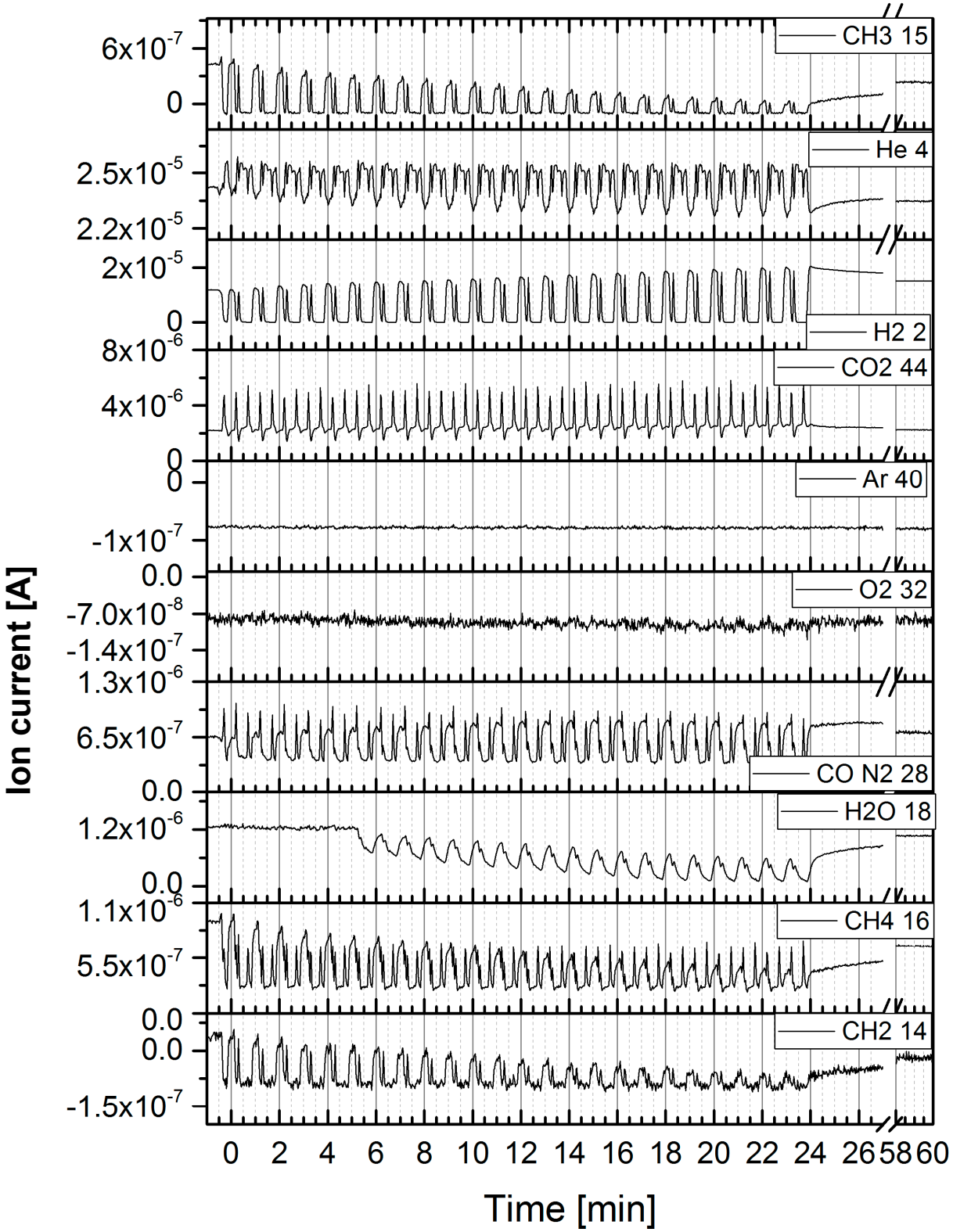

Figure S14. Full MS data set recorded during the 30 s H_2 dropout modulations.

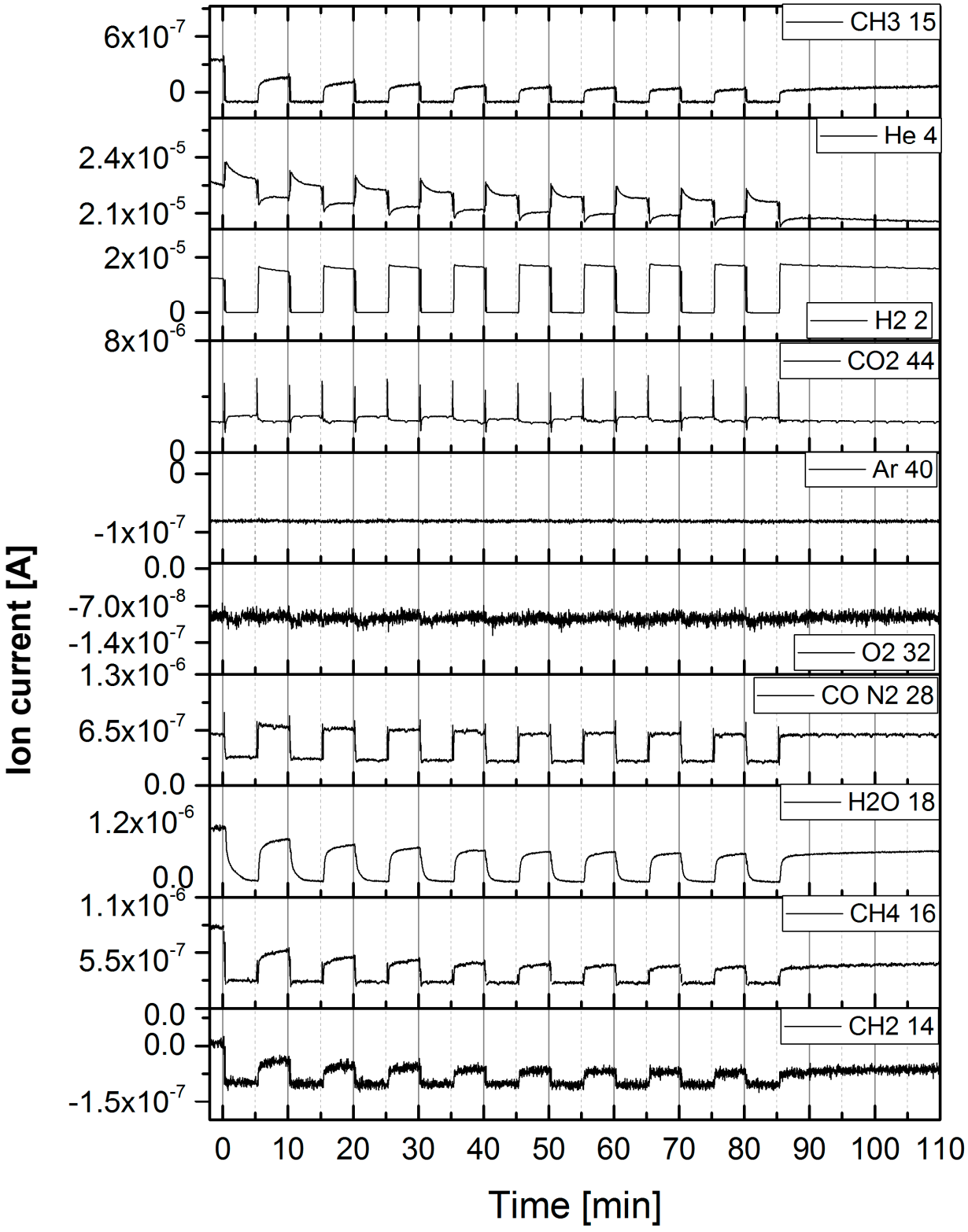

Figure S 15. Full MS data set recorded during the 300 s H_2 dropout modulations.

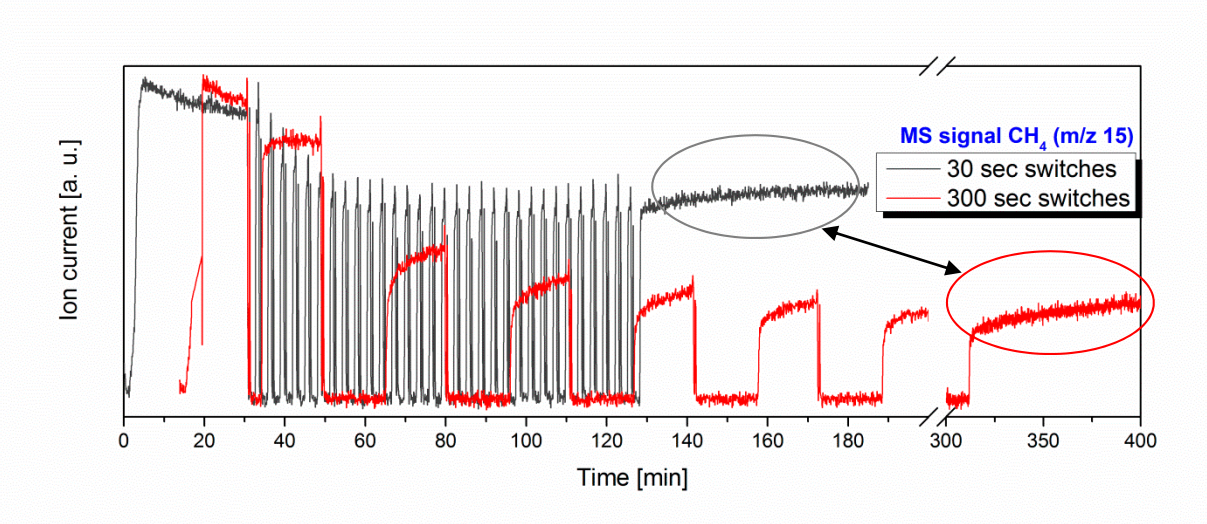

Figure S16. MS data during both the 30 s (black) and 300 s (red) modulation.

In both experiments, a similar activity to CH_4 was obtained over the Ni catalyst. After the modulations with different length, different activity was observed (300 s modulations led to stronger deactivation).

4. Additional H_2 modulation experiments

60 s H_2 dropout modulation experiment in the absence of O_2 using short and thin stainless steel tubing and a CO_2 (99.998%) bottle directly placed next to the mass flow controllers (Figure S17). The experiment showed a CH_4 signal in the MS on a stable level and no catalyst deactivation.

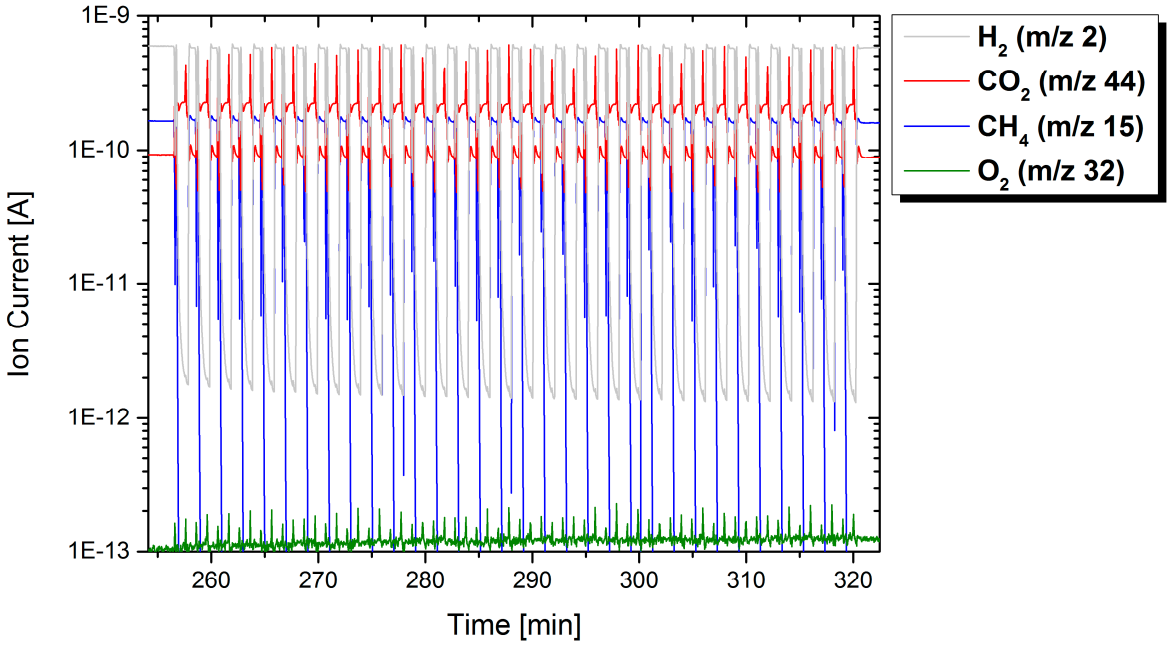

Figure S17. Methanation of CO_2 during dynamic operation switching every 60 s between methanation conditions ($H_2/CO_2 = 4$) and CO_2 at constant WHSV of 12000 $mL_{CO2}/(g_{cat} \cdot h)$ and GHSV of 71700 h^{-1} using the 10 wt% Ni/Al_2O_3 catalyst in an O_2 free experiment (quartz glass capillary). The figure shows the MS signals of H_2, CO_2, CH_4 and O_2.

Periods of 300 s of H_2 dropouts were performed in a lab-scale reactor under similar reaction conditions (WHSV = 12000 $mL_{CO2}\ g_{cat}^{-1}\ h^{-1}$) as in the *operando* QEXAFS experiments. The 10 wt% Ni/Al_2O_3 catalyst was exposed to a series of H_2 dropout periods intensified with 300–500 ppm O_2 to induce fast

and deep oxidation and deactivation of the catalyst (Figure S18). The initial activity of the catalyst (cycle 1) resulted in a conversion of CO_2 of 68% with a selectivity of 96% towards CH_4. The first two H_2 dropout periods containing 300 ppm O_2 caused only minor deactivation of the catalyst leading to a CO_2 conversion of 66% (cycle 2) and 64% (cycle 3) and a decline in selectivity to 94% (cycle 2) and 92% (cycle 3). A more pronounced deactivation was observed when 500 ppm O_2 were dosed during the H_2 dropout periods. The conversion of CO_2 declined to 57% (cycle 4) and further to 41% (cycle 5) and the selectivity towards CH_4 also decreased significantly to 82% (cycle 4) and 61% (cycle 5). Full oxidation of the catalyst was suspected during the fourth H_2 dropout indicated by a strong increase of the O_2 signal in the MS (Figure S18 (b)). This observation implies that Ni is fully transformed to NiO and O_2 is not consumed for oxidation anymore. Full Ni oxidation during H_2 dropouts is in line with the *operando* QEXAFS experiments.

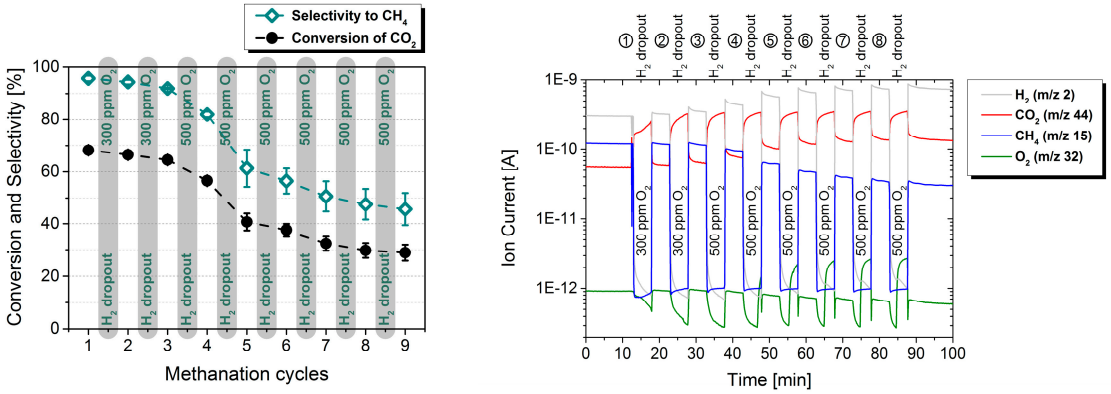

Figure S18. Series of 300 s H_2 dropout periods during the methanation of CO_2 containing 300–500 ppm O_2 using the 10 wt% Ni/Al_2O_3 catalyst; conditions: stainless steel tubular fixed-bed reactor, 150 mg catalyst, $H_2/CO_2 = 4$ diluted in 75% N_2 or 5% CO_2 / N_2 + 300–500 ppm O_2, p=1 atm, T=400 °C, GHSV = 26700 h^{-1} and WHSV = 12000 mL_{CO2} g_{cat}^{-1} h^{-1}. GC data (a) and corresponding MS data (b).

References

1. Calvin, S.; Carpenter, E.; Ravel, B.; Harris, V.; Morrison, S. Multiedge refinement of extended X-ray-absorption fine structure of manganese zinc ferrite nanoparticles. *Phys. Rev. B: Condens. Matter* **2002**, *66*, 224405.